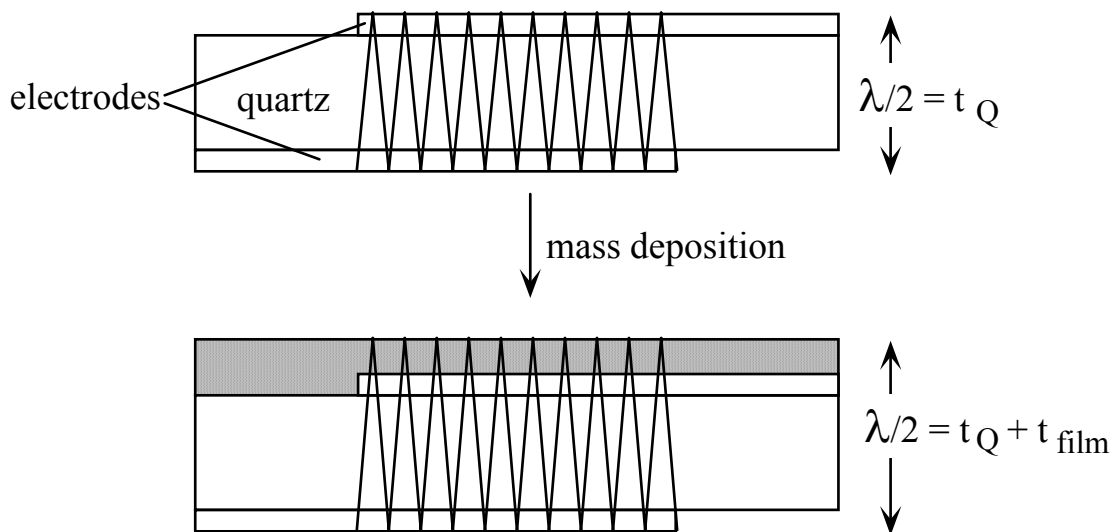


## Quartz Crystal Microbalance Research

In the last decade, a new analytical method for the *in situ* investigation of interfacial processes, including electrode processes, has emerged. This method, commonly referred to as the quartz crystal microbalance (QCM), has had a significant impact in numerous research programs. This includes electrochemists, for which the method is referred to as the electrochemical quartz crystal microbalance (EQCM). These methods rely on the piezoelectric properties of quartz, in particular a single crystal of quartz that has been cut into a thin wafer at an angle of approximately 35 degrees with respect to the polar z-axis of quartz. The word piezoelectric derives from the word *piezein*, meaning to press. Hence, the piezoelectric effect hinges on "pressure electricity," a phenomenon first observed by Jacques and Pierre Curie when they discovered that mechanical stress applied to the surfaces of certain crystals, including quartz, resulted in an electrical potential across the crystal. Shortly afterward, the converse piezoelectric effect – a mechanical strain produced by application of a electric potential across the crystal – was discovered. This effect is sometimes referred to as the converse piezoelectric effect. The motor generator properties have long been associated with underwater sound transducers (sonar), and electromechanical devices such as speakers, microphones, and phonograph pickups.

The quartz crystal microbalance earns its name from its ability to measure the mass of thin films that have adhered to its surface. The quartz crystal microbalance generally comprises a thin AT-cut quartz wafer with a diameter of 0.25 - 1.0 inches, sandwiched between two metal electrodes which are used to establish an electric field across the crystal. If an alternating electric field and appropriate electronics are used, the crystal can be made to oscillate at its resonant frequency. Most crystals of current interest resonate between 5 to 30 MHz. The measured frequency is dependent upon the combined thickness of the quartz wafer, metal electrodes, and material deposited on the quartz crystal microbalance surface. Because the resonance is very sharp, high precision frequency measurements allow the detection of minute amounts of deposited material, as small as 100 picograms on a square centimeter. Mass changes occurring at the QCM surface result in frequency changes according to the well established Sauerbrey equation, named after the pioneer of this technique for measurement of film thickness.



The Sauerbrey equation:

$$\Delta f = \frac{-2f_0^2 \Delta m}{A\sqrt{\mu_Q\rho_Q}}$$

where  $f_0$  is the resonant frequency of the quartz resonator,  $\Delta m$  is the mass change,  $A$  is the active vibrating area,  $\mu_Q$  is the shear modulus of quartz, and  $\rho_Q$  is the density of quartz.

Early applications of the quartz crystal microbalance involved the well-documented measurement of metal deposition in high-vacuum metal evaporators, which is still widely practiced. This allows for real-time, rapid measurement of film thicknesses with Angstrom resolution. Advances in quartz crystal microbalance methodology in the last decade now allow for dynamic measurements of minute mass changes at surfaces, thin films and electrode interfaces prepared on the quartz crystal, while the surface is immersed in liquid. The capability for direct, real-time, highly sensitive mass measurement in the liquid phase offers opportunities not available by other means. Recent developments also have illustrated that the quartz crystal microbalance is capable of measuring the viscosity and density of liquids near the quartz crystal microbalance surface. Combining this technique with electrochemical instrumentation allows simultaneous measurement of mass and electrochemical variables such as electrochemical potential, current and charge. The EQCM has emerged as a powerful technique capable of detecting very small mass changes at the electrode surface that accompany electrochemical processes. This relatively simple technique only requires, in addition to conventional electrochemical equipment, an inexpensive radiofrequency oscillator, a frequency counter, and commercially available AT-cut quartz crystals.

The quartz crystal microbalance has been used for a variety of applications in our group, including mass changes at electrode surfaces during deposition, measurements of changes in the composition of depletion layers during cyclic voltammetry, measurement of surfactant enhanced spreading of ultrathin aqueous films, measurement of contact angles, and rheology of thin polymer films.

#### Electrochemical Quartz Crystal Microbalance

An AT-cut quartz crystal can be interfaced with conventional electrochemical apparatus so that mass changes occurring at the electrode surface during electrochemical processes can be directly monitored. This method is now practiced routinely in numerous laboratories. The construction of an EQCM is relatively simple and inexpensive, requiring a frequency counter, a dual-voltage power supply, a potentiostat, a voltmeter, appropriate cabling and assembly of an oscillator circuit. For a complete manifest of the required components, schematics of the oscillator circuit, and the hardware necessary for QCM and EQCM, [click here](#).

#### **Some representative publications**

##### QCM Sensors and Biosensors

- Amplified Mass Immunosorbent Assay with a Quartz Crystal Microbalance, M. D. Ward and R. C. Ebersole, *J. Amer. Chem. Soc.*, **110**, 8623, **1988**.

- Spontaneously Formed Functionally Active Avidin Monolayers on Metal Surfaces: A Strategy for Immobilizing Biological Reagents and Design of Piezoelectric Biosensors, R. C. Ebersole, J. R. Moran and M. D. Ward, *J. Amer. Chem. Soc.*, **112**, 3239, **1990**.
- Piezoelectric Cell Growth Sensor, R. C. Ebersole, R. P. Foss and M. D. Ward, *Bio/Technology*, **1991**, 9, 450.
- Piezoelectric pH Sensors: AT-cut Quartz Resonators with Amphoteric Polymer Films, J. Wang, M. D. Ward, R. C. Ebersole and R. A. Foss, *Analytical Chemistry*, **1993**, 65, 2553.
- Piezoelectric Detection of Anchorage-Dependent Cell Mass Changes, D. Gryte, M. D. Ward and W.-S. Hu, *Biotechnol. Prog.* **1993**, 9, 105.

#### Helpful Review Articles

- In-situ Interfacial Mass Measurements with Piezoelectric Transducers: Fundamentals and Applications, M. D. Ward and D. A. Buttry, *Science*, **249**, 1000, **1990**.
- Measurement of Interfacial Processes at Electrode Surfaces with the Electrochemical Quartz Crystal Microbalance, *Chemical Reviews* (invited review), D. A. Buttry and M. D. Ward, **1992**, 92, 1355.
- Principles and Applications of the Electrochemical Quartz Crystal Microbalance, M. D. Ward, *Monographs in Electroanalytical Chemistry and Electrochemistry: Physical Electrochemistry, Principles, Methods, and Applications*, I. Rubinstein, Ed., **1995**, Marcel Dekker, New York.

#### Fundamental Properties

- Radial Sensitivity of the Quartz Crystal Microbalance in Liquid Media, M. D. Ward and E. J. Delawski, *Anal. Chem.*, **1991**, 63, 886.
- Scanning electrochemical mass sensitivity mapping of the quartz crystal microbalance in liquid media, A. C. Hillier and M. D. Ward, *Anal. Chem.* **1992**, 64, 2539.
- Self-assembled Thiol Monolayers with Carboxylic Acid Functionality: Measuring pH-Dependent Phase Transitions with the Quartz Crystal Microbalance, J. Wang, L. M. Frostman and M. D. Ward, *J. Phys. Chem.* **1992**, 96, 5224.
- Depletion Layer Effects on the Response of the Electrochemical Quartz Crystal Microbalance, W.-W. Lee, H. S. White and M. D. Ward, *Anal. Chem.*, **1993**, 65, 3232.
- The Role of Longitudinal Waves in Quartz Crystal Microbalance Applications in Liquids, Z. Lin and M. D. Ward, *Anal. Chem.*, **1995**, 34, 685.
- Probing Solvent Dynamics in Concentrated Polymer Films with a High Frequency Shear Mode Quartz Resonator, A. Katz and M. D. Ward, *J. Appl. Phys.*, **1996**, 80, 4153.

#### Miscellaneous Applications

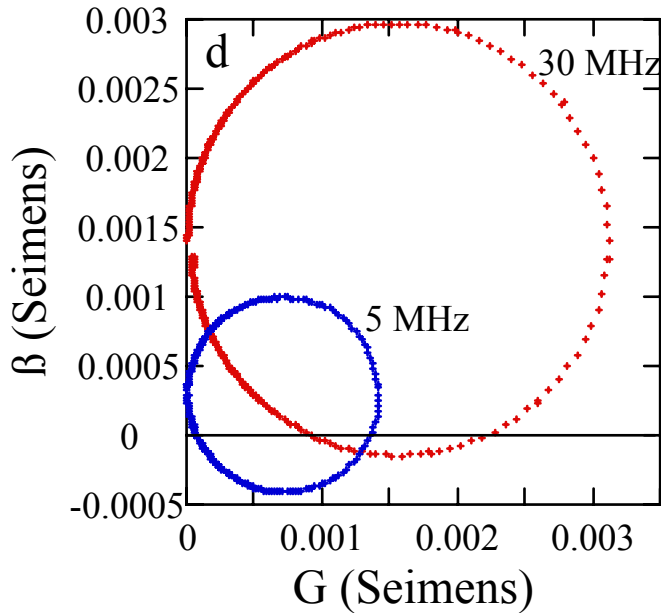
- Operation of an Ultrasensitive 30 MHz Quartz Crystal Microbalance in Liquids, Z. Lin, C. M. Yip, I. S. Joseph and M. D. Ward, *Analytical Chemistry*, **1993**, 65, 1646.
- Probing Electrocrystallization of Charge Transfer Salts with the Quartz Crystal Microbalance, *J. Electroanal. Chem.*, **273**, 79, **1989**.
- Electrochemical and Quartz Crystal Microbalance Evidence for Mediation and Direct Electrochemical Reactions of Small Molecules at Tetrathiafulvalene-tetracyanoquinodimethane (TTF-TCNQ) Electrodes, M. S. Freund, A. Brajter-Toth and M. D. Ward, *J. Electroanal. Chem.*, **289**, 127, **1990**.
- Determination of Wetting Velocities of Surfactant Superspreaders with the Quartz Crystal Microbalance, Z. Lin, R. M. Hill, H. T. Davis, and M. D. Ward, *Langmuir*, **1994**, 10, 4060.

- Improved Accuracy in Dynamic Quartz Crystal Microbalance Measurements of Surfactant Enhanced Spreading, Zuxuan Lin, T. Stoebe, Randal M. Hill, H. Ted Davis, and Michael D. Ward, *Langmuir*, **1996**, *12*, 345.
- Determination of Contact Angles and Surface Tensions with the Quartz Crystal Microbalance, Zuxuan Lin and Michael D. Ward, *Analytical Chemistry*, **1996**, *68*, 1285.

#### Ultrasensitive 30 MHz Quartz Crystal Microbalance

- Operation of an Ultrasensitive 30 MHz Quartz Crystal Microbalance in Liquids, Z. Lin, C. M. Yip, I. S. Joseph and M. D. Ward, *Analytical Chemistry*, **1993**, *65*, 1646.

A new ultrasensitive quartz crystal microbalance (QCM), based on 30 MHz AT-cut shear mode crystals, for operations in gas and liquid phases, was described by our group. In liquid media, a linear relationship between  $\Delta f$  and  $(\eta_L \rho_L)^{1/2}$  was observed, in agreement with theory. Impedance analyses also showed a linear dependence of equivalent resistance on  $(\eta_L \rho_L)^{1/2}$ . The capabilities of these resonators in electrochemical QCM (EQCM) applications was demonstrated by the electrodeposition of copper at the QCM surface. Simultaneous measurements of frequency and charge afforded sensitivity constants that were in exact agreement with theory, indicating that energy trapping of the fundamental mode is very efficient for the 30 MHz resonators. The high sensitivity of these devices portends their use in applications such as miniature viscometers, chemical and biological sensors, and for fundamental investigations of interfacial processes. These results also suggest that miniaturization and microfabrication of shear mode devices, which will require thinner quartz crystals operating at high frequency, can be accomplished with retention of stability. In fact, admittance analysis indicated that the 30 MHz resonators have better performance characteristic than the 5 or 10 MHz crystals typically used in liquid applications. The capacitance of the 30 MHz resonator is greater because of their decreased thickness, resulting in an upwards shift of the admittance locus. If this shift is too large the locus may not cross the real axis (conductance), which is required for achieving stable resonance in the feedback circuit during conventional operation. However, the 30 MHz crystals are thinner than the lower frequency crystals and therefore have less energy dissipation. This results in an increase in the diameter of the admittance locus such that it crosses the real axis at a higher conductance than 5 MHz crystals. Consequently, the 30 MHz crystals actually are more stable during operation. These crystals are available from Piezo Technology, Inc. (Orlando, Florida).



Admittance plots for the 5 MHz and 30 MHz QCMs in water.

Probing the Depletion Layer with the EQCM

- Depletion Layer Effects on the Response of the Electrochemical Quartz Crystal Microbalance, W.-W. Lee, H. S. White and M. D. Ward, *Anal. Chem.*, **1993**, *65*, 3232.

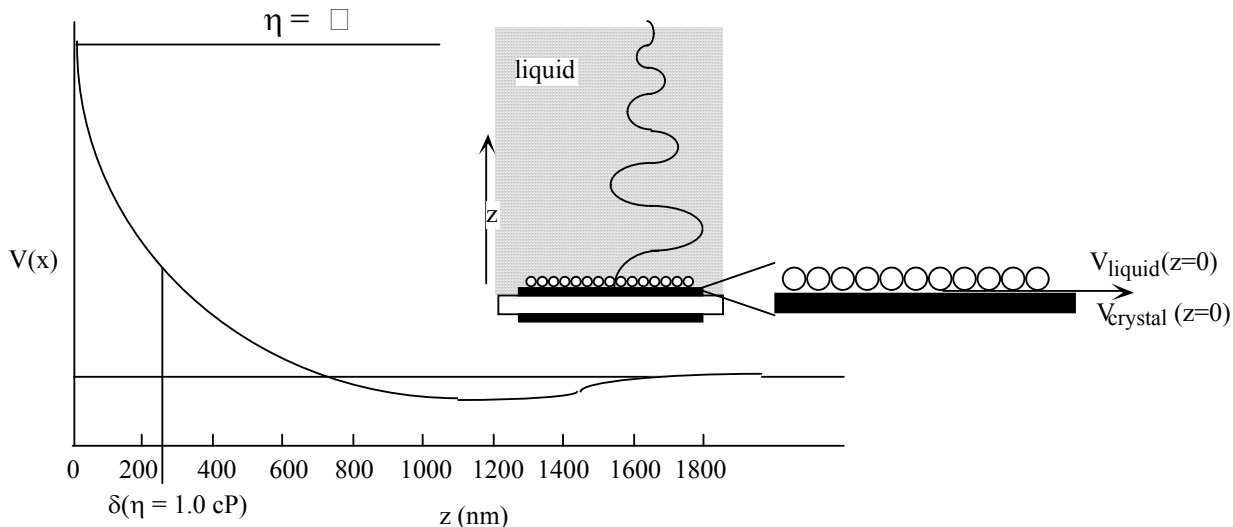
Because the resonant frequency of the quartz crystal microbalance is sensitive to the density and viscosity of the fluid in contact with its surface, measurements of mass changes at electrodes with the EQCM require attention to changes in the viscosity and density of the depletion layer that may accompany redox processes. The quartz resonator frequency depends on density ( $\rho$ ) and viscosity ( $\eta$ ) according to

$$\Delta f = -f_0^{3/2} \left( \frac{\rho_L \eta_L}{\pi \rho_Q \mu_Q} \right)^{1/2}$$

and the decay length of the shear wave can be calculated by

$$\delta = \sqrt{\frac{\eta_L}{\pi f_0 \rho_L}}$$

for which the velocity decays according to  $V_x(z,t) = Ae^{-kz} \cos(kz - \omega t)$ .



Schematic representation of the decay of an acoustic shear wave emanating from the QCM surface in a Newtonian fluid.

The thickness of the depletion layer resulting from voltammetric oxidation or reduction of an electroactive species is approximately equal to  $(Dt)^{1/2}$ , where  $D$  is the diffusion constant and  $t$  is the characteristic time of the experiment ( $t \approx RT/Fn$  for cyclic voltammetry). Changes in density and viscosity can be expected if the concentration of counterions changes appreciably, if the product is chemically reactive, or if the product undergoes large conformational or solvation changes following electron transfer. These effects will be more pronounced when the concentrations of the reactants and products are large. A 0.1% change in  $(\eta\rho)^{1/2}$  will result in a 7.4 Hz shift for a 5 MHz EQCM. Since many EQCM measurements involve minute mass changes, interference from this effect must be considered in any experiment.

Changes of  $\eta$  and  $\rho$  in the depletion layer were illustrated by the EQCM response during cyclic voltammetry of the ferri/ferrocyanide redox couple. The physical origin of the effect is the larger number of counterions associated with  $\text{Fe}(\text{CN})_6^{4-}$  compared to  $\text{Fe}(\text{CN})_6^{3-}$ , leading to lower frequencies when the depletion layer contains the former. The observed response is nominally identical to that predicted by computer simulation, which were based on average values of  $\eta$  and  $\rho$  determined during the digital simulation by weighting of the calculated values of  $\rho(z)$  and  $\eta(z)$  with the exponential term  $e^{-z/\delta}$ . This treatment accounts for the decreasing sensitivity to  $\rho$  and  $\eta$  with increasing  $z$  (distance from the quartz resonator surface), which results from the decreasing amplitude of the shear wave with a decay length  $\delta$ . This exponential weighting function physically simulates the exponential decay of the shear wave emanating from the surface of the EQCM. The depletion layer thickness in a typical cyclic voltammetry measurement exceeds 100  $\mu\text{m}$ , substantially greater than  $\delta$ . Consequently, the frequency measured at the extremes of the potential cycle, in the mass transport limited region, is representative of the properties within the entire depletion layer. These effects need to be considered when a modest concentration (20 - 100 mM) of redox species is present. Under conditions where migration is important the contribution from this effect can be even more significant as the oxidation or reduction of a soluble electroactive species can result in the accumulation of larger excess quantities of counterions within the depletion layer.

### Measuring Spreading of Ultrathin Water Films on the QCM

- Determination of Wetting Velocities of Surfactant Superspreaders with the Quartz Crystal Microbalance, Z. Lin, R. M. Hill, H. T. Davis, and M. D. Ward, *Langmuir*, **1994**, *10*, 4060.
- Improved Accuracy in Dynamic Quartz Crystal Microbalance Measurements of Surfactant Enhanced Spreading, Zuxuan Lin, T. Stoebe, Randal M. Hill, H. Ted Davis, and Michael D. Ward, *Langmuir*, **1996**, *12*, 345.

The radial sensitivity of the quartz crystal microbalance (QCM), comprising an AT-cut quartz crystal coated with gold electrodes, was exploited for the measurement of wetting rates of aqueous dispersions of a trisiloxane surfactant exhibiting "superspreading" behavior on different surfaces. The rate at which a droplet advances across the QCM surface was measured directly from the frequency transient accompanying radial spreading of the drop from the center of the quartz crystal to the periphery. This method provides for convenient measurement of spreading rates under a variety of conditions, allowing systematic investigations of the wetting behavior dependence on surfactant concentration, substrate surface energy, and humidity. The substrate surface energy can be adjusted readily by the preparation, on the gold electrodes of the QCM, of self-assembled single component or mixed organosulfur monolayers with judiciously chosen chemical functionalities at the termini of the alkyl chains. The surfactant concentration at which the maximal spreading velocity occurred was independent of substrate surface energy, indicating that the spreading rate was dependent upon the microstructure of the surfactant dispersion rather than the energetics of the solution/substrate interface. These studies also revealed a surprising dependence of the wetting velocity on surface energy in which the velocities were greatest on surfaces of moderate hydrophobicity. Previous work indicated that superspreading required a humid environment, suggesting that a thin film of water on the hydrophobic surface was required. The studies described here revealed significant water condensation on rough hydrophobic QCM surfaces compared to smooth hydrophobic surfaces, which is attributable to capillary condensation on the rough surfaces. Consequently, superspreading was observed on rough surfaces of high hydrophobicity, but is negligible on smooth ones. The resolution of the preexisting water film issue, and the heretofore undiscovered influence of surface energy on superspreading, demonstrated the utility of the QCM for measurements of dynamic wetting behavior.

These studies were followed by an improvement in the methodology which provided for more accurate spreading rates. The modification involved larger QCM electrodes, which increased the area over which the spreading event was measured compared to previously used smaller electrodes, and a frequency counter capable of more rapid data acquisition. The larger electrodes permitted spreading to be measured for longer times over a larger area relative to the initial drop size, while faster data acquisition provided more data immediately following introduction of the droplet to the QCM surface. This obviated overweighting of data acquired in the later stages of spreading when the aqueous film approached the electrode edges and advanced along the electrode tabs. These wetting rates were corroborated by real-time video microscopy of the wetting processes on identical surfaces. Comparison of the wetting rates on gold electrodes modified with various organosulfur monolayers revealed that the dependence of rates on surface energy is identical for the different electrode sizes, the rates being systematically larger for the larger electrodes.

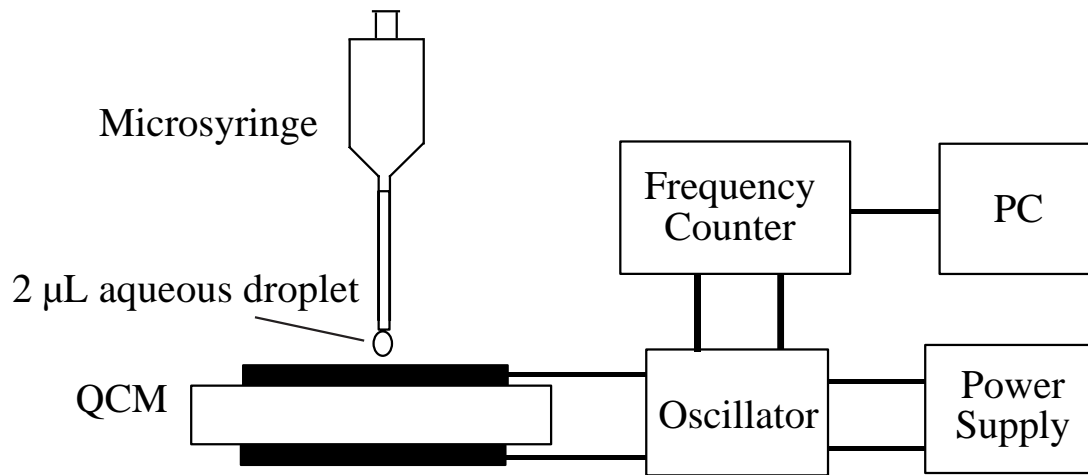
The quartz resonator frequency depends on density ( $\rho$ ) and viscosity ( $\eta$ ) according to

$$^2 f = -f_0^{3/2} \left( \frac{\rho_L \eta_L}{\pi \rho_Q \mu_Q} \right)^{1/2}$$

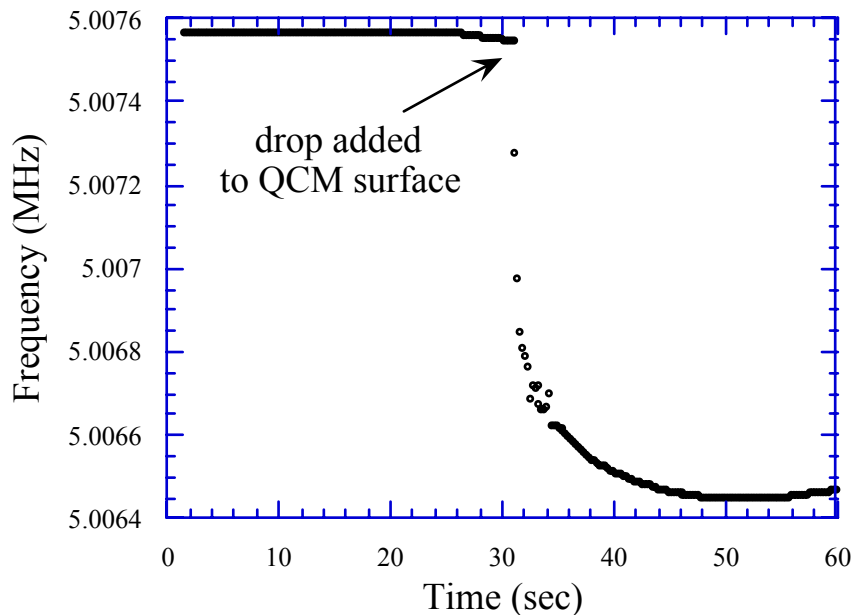
and the decay length of the shear wave is given by

$$\delta = \sqrt{\frac{\eta_L}{\pi f_0 \rho_L}}$$

for which the velocity decays according to  $V_x(z,t) = Ae^{-kz}\cos(kz-\omega t)$ . Consequently, the microbalance measures the advance of the ultrathin water film by detecting the mass of the film contained with a thickness approximately equal to the decay length  $\delta$  as it spreads over an increasing area of the actively vibrating region.



Schematic representation of the experimental apparatus used to administer aqueous drops to the QCM surface. The liquid is administered to the center of the resonator by striking, with a mechanical drop knocker, the glass capillary tip at the end of the syringe. The QCM frequency is monitored continually while the drop spreads from the center to the outer edges.



Typical frequency transient for the radial spreading of an aqueous films on the QCM. The liquid mass is constant throughout the spreading process, but the viscous loss encountered by the shear wave in the liquid results in velocity decay from the maximum amplitude at  $z = 0$  to  $1/e$  of this value at  $\delta$ , the decay length. Consequently, only the mass contained within the decay length is detected. Upon administration of a liquid drop to the center of the resonator the frequency decreases, and as the mass spreads toward the outer regions of the resonator the frequency decreases further at a rate dictated by the spreading velocity and the sensitivity profile of the QCM.

#### Measuring Contact Angles with the QCM

- Determination of Contact Angles and Surface Tensions with the Quartz Crystal Microbalance, Zuxuan Lin and Michael D. Ward, *Analytical Chemistry*, **1996**, 68, 1285.

A method based on the quartz crystal microbalance (QCM) for measuring the sessile contact angles and surface energies of liquid-air and liquid-liquid interfaces is described. The method involves measurement of the frequency change accompanying the introduction of a small liquid droplet to the center of a vibrating quartz resonator, which comprises an AT-cut quartz crystal sandwiched between two gold electrodes. If the density and viscosity of the liquid are known, the contact angle between the droplet and the gold substrate surface can be determined directly. QCM measurements of contact angles formed between aqueous droplets and gold surfaces modified with various organosulfur monolayers having different surface energies agree with sessile contact angles determined by optical goniometry. Furthermore, the QCM method can be used to measure the contact angle formed between an aqueous droplet and the QCM surface when both are submerged under an immiscible solvent such as hexadecane. In this case, the frequency change relies on the differences in the densities and viscosities of the water droplet and the fluid displaced by the droplet at the surface. The dependence of the contact angle on the concentration of surfactant in the aqueous droplet provides for determination of the critical

micelle concentration for aqueous phases in contact with air or an immiscible organic fluid. These measurements can be performed under conditions where contact angles cannot be measured readily, such as in the presence of opaque media or in the case of two liquids having similar refractive indexes.

For the numerical analysis program used to determine the contact angle from the QCM measurement go to our [software](#) page.

### Rheology of Thin Polymer Films

- Probing Solvent Dynamics in Concentrated Polymer Films with a High Frequency Shear Mode Quartz Resonator, A. Katz and M. D. Ward, *J. Appl. Phys.*, **1996**, *80*, 4153.

Solvent reorientational dynamics in concentrated polymer films have been probed with a new experimental method based on a linear electromechanical model and a AT-cut high frequency quartz resonator. This method is unique in that the viscoelastic characteristics of a composite resonator comprising the viscoelastic film and the quartz resonator are probed at the frequency of minimum resonator amplitude ( $f_{Ymin}$ ) rather than at  $f_{Ymax}$ , thus permitting measurements under conditions where a linear electromechanical model is most applicable. The method involves measurement of the admittance characteristics of the unloaded quartz resonator and the composite resonator, transformation of the admittance data near  $f_{Ymin}$  into a linear form that provides accurate determination of the resonant conductance and susceptance, and use of Newton-Raphson numerical iteration to determine the viscoelastic characteristics from these values. This procedure enables real-time investigation of dynamic processes in polymer films, as demonstrated here by the simultaneous determination of the film thickness, storage modulus and loss modulus during the drying of a spin-coated film containing polystyrene and 2-chlorotoluene solvent. The viscoelastic characteristics are investigated at a resonant frequency near 5 MHz under ambient conditions as the solvent mass fraction continuously decreases from its initial value of 15%. The trends in the measured storage and loss moduli are consistent with a single relaxation process, namely rotational relaxation of the 2-chlorotoluene solvent molecules. The solvent relaxation time increases with decreasing solvent content owing to the increasing influence of the polymer chains on the solvent reorientational dynamics. A plateau in the relaxation time at low solvent content (< 2%) suggests the presence of a solvent glass transition. The results demonstrate that shear mode quartz resonators can be used to investigate solvent dynamics in polymer films at high concentrations that are inaccessible by other experimental methods.

$Y = (G + i\beta) @ \text{resonant frequency} =$

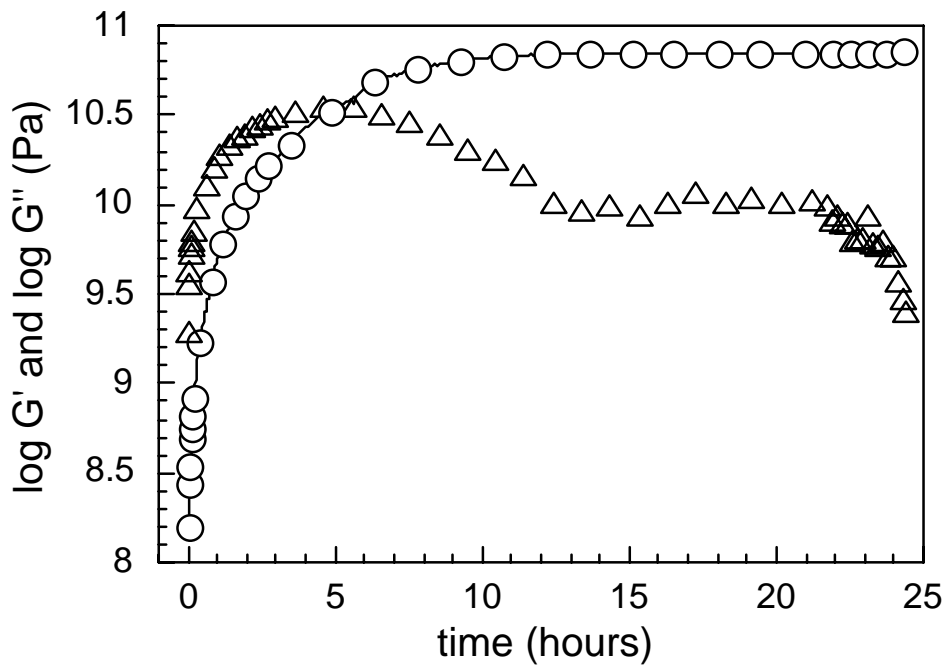
$$\frac{i\omega A_{act} \varepsilon_{22}}{l_q} (\mathbf{k}_q \bar{c}_{66} \sin(\mathbf{k}_q l_q) + \mathbf{k}_L \bar{\mu}_L \tan(\mathbf{k}_L l_L) \cos(\mathbf{k}_q l_q))$$


---

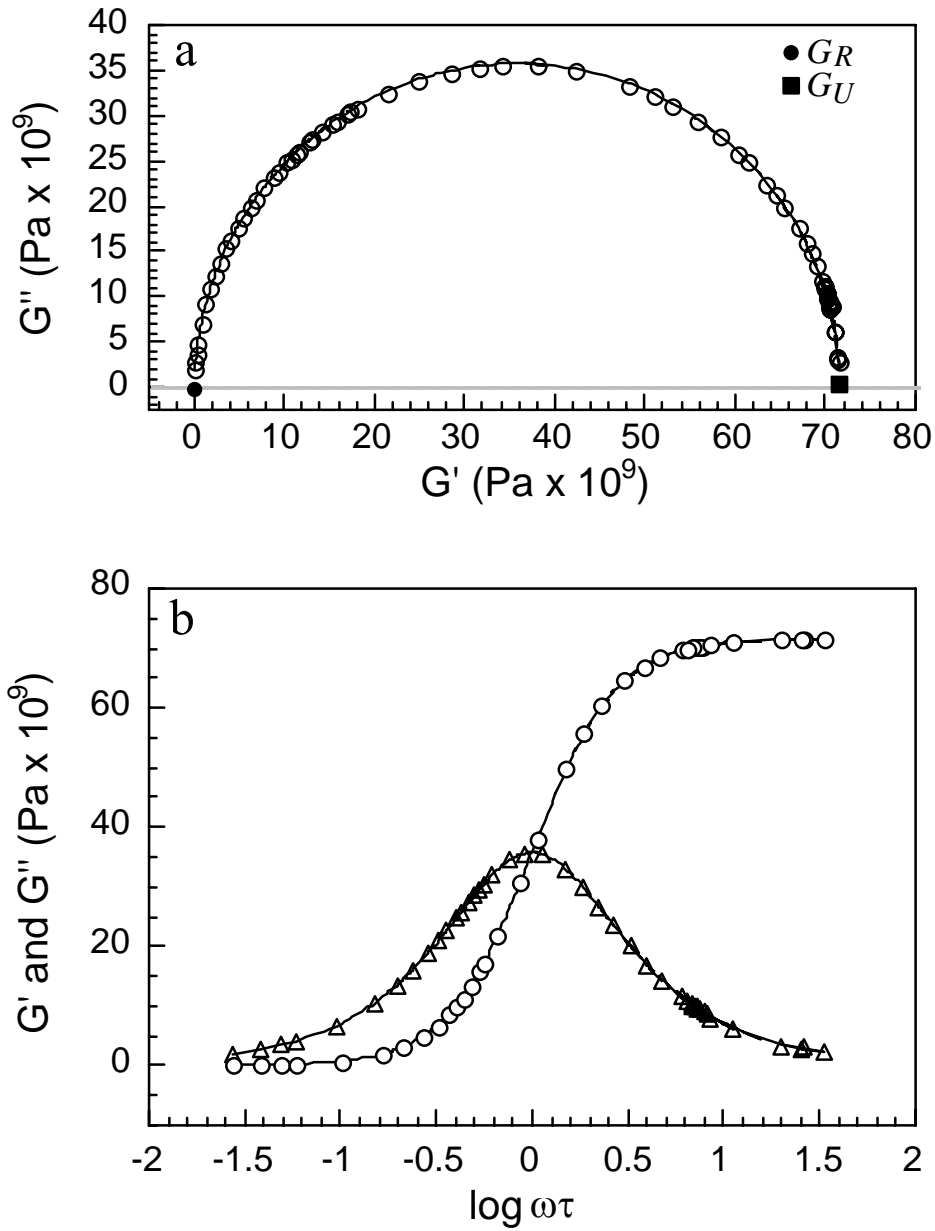

$$\mathbf{k}_q \bar{c}_{66} \sin(\mathbf{k}_q l_q) + \mathbf{k}_L \bar{\mu}_L \tan(\mathbf{k}_L l_L) \cos(\mathbf{k}_q l_q) - \frac{2e_{26}^2}{l_q \varepsilon_{22}} [1 - \cos(\mathbf{k}_q l_q)] + \frac{\mathbf{k}_L \bar{\mu}_L}{2k_q \bar{c}_{66}} \tan(\mathbf{k}_L l_L) \sin(\mathbf{k}_q l_q)]$$

$$\mathbf{k}_q = \omega \sqrt{\frac{\rho_q}{c_{66} + \frac{e_{26}^2}{\epsilon_{22}} + i\omega\eta_q}} = \omega \sqrt{\frac{\rho_q}{\underline{\underline{c_{66}}}}}$$

$$\mathbf{k}_L = \omega \sqrt{\frac{\rho_L}{\mu_L + i\omega\eta_L}} = \omega \sqrt{\frac{\rho_L}{\underline{\underline{\mu_L}}}}$$



Moduli  $G'$  and  $G''$  measured during the loss of *o*-chlorotoluene from a thin polystyrene film coated on a QCM, as measured with the admittance analysis method.

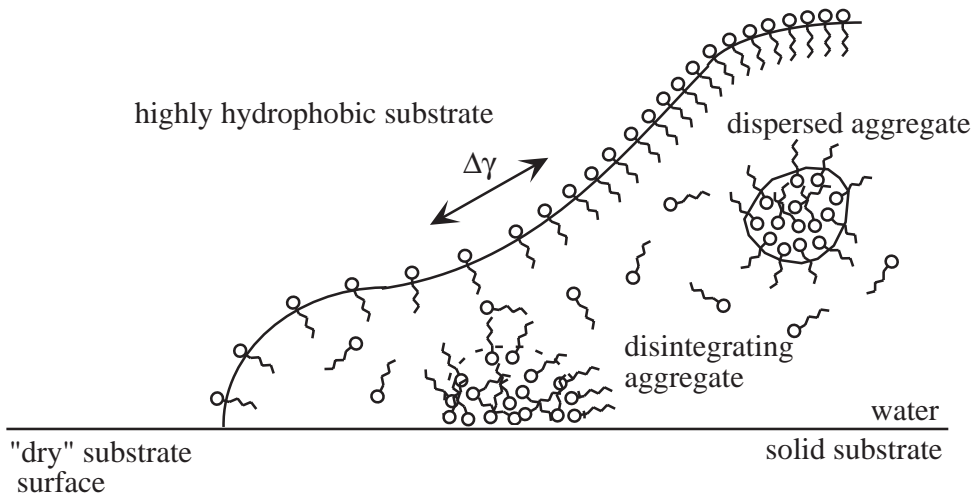
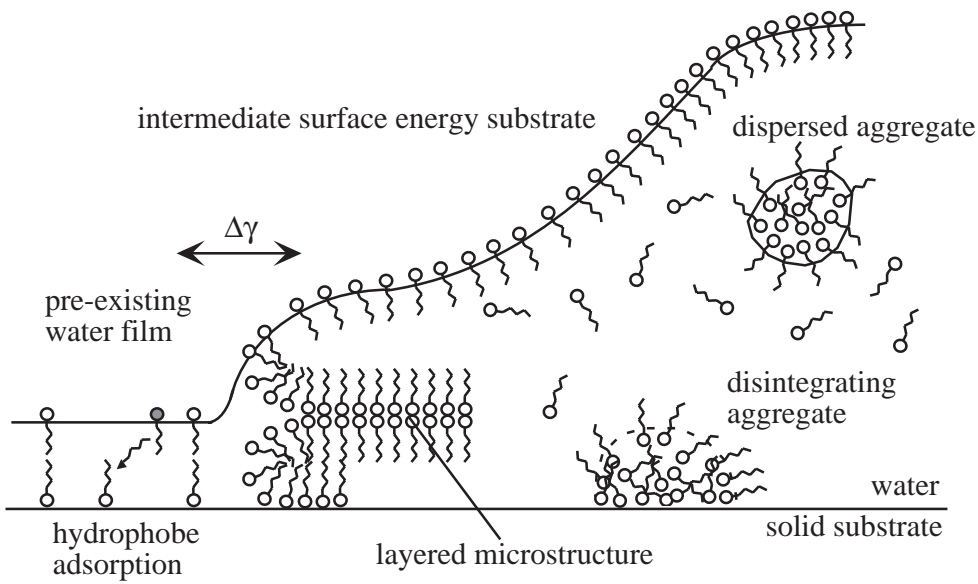
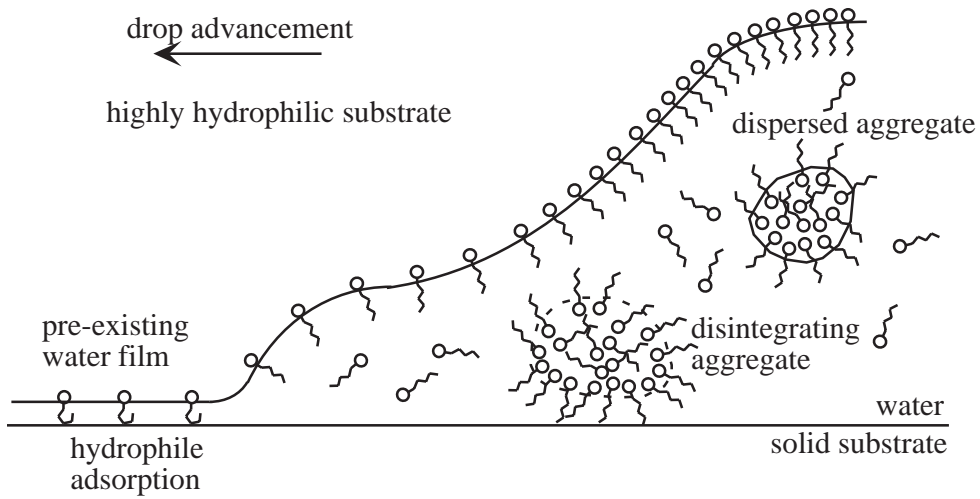


The  $G''$  and  $G'$  data in (a) and (b), obtained by admittance analysis are indicative of the measurement of a process characterized by a single relaxation time, even though in (b) it is clear that the measurement was performed over an effective frequency range spanning three orders of magnitude. These experiments revealed that the quartz resonator was actually probing the relaxation of the o-chlorotoluene solvent molecules in the polymer film. Nevertheless, the increasing rigidity of the polymer film can be surmised from the decreasing solvent relaxation time as the film dries.

### Research on Surfactant Enhanced Spreading

Our group, in collaboration with H. T. Davis (Chemical Engineering and Materials Science, University of Minnesota) and Randall M Hill (Dow Corning) has made significant contributions to the understanding of “Surfactant Enhanced Spreading.” This phenomenon refers to the ability of specific surfactants to promote the spreading of an aqueous film on a surface that does not support spreading in the absence of the surfactant. Our efforts have revealed several key aspects of this process:

- (1) Surfactant enhanced spreading is a general phenomenon as it is observed for a variety of nonionic surfactants and certain ionic surfactants;
- (2) The observation of the surfactant enhanced spreading is substrate dependent,
- (3) The phenomena is characterized by a maximum spreading rate at a specific substrate surface energy, the location of this maximum dependent upon the surfactant and related roughly to the relative amount of the hydrophobic and hydrophilic segments in the surfactant.
- (4) The data indicate that spreading on low surface energy substrates is promoted by Marangoni flow associated with the surface tension gradient between the surfactant-rich droplet added to the substrate surface and a preexisting water film on the surface.
- (5) The data indicate that spreading on high energy substrates is retarded because of adsorption of the hydrophilic surfactant segment, which then results in the hydrophobic segment presenting at the surface and retardation of advancement of the aqueous film.
- (6) The evidence points to a role for lamellar phases that can deliver surfactant rapidly to the air-liquid interface near the advancing edge of the aqueous film.



The figure above is a schematic representation of the processes that may be responsible for surfactant enhanced spreading. In (a) and (b) the drop introduced to the surface actually is in contact with a pre-existing water layer. The contact line defining the boundary of the leading edge of the droplet and the pre-existing water layer is continuous and may not be very distinct. However, the surfactant concentrations at the air-water interfaces of the droplet and the region just beyond this contact line will differ throughout the spreading event due to continuous advancement of the contact line across the pre-existing water layer, which initially is devoid of surfactant. A surface tension gradient ( $\Delta\gamma$ ) between a pre-existing water layer and the surfactant/water droplet favors Marangoni flow and rapid spreading of the aqueous droplet. (a) On highly hydrophilic substrates the pre-existing water layer will be present. However, spreading on these surfaces is observed to be slow. This can be attributed to adsorption of the surfactant hydrophiles on the substrate, which forces the hydrophobe to point away from the substrate surface and presents a hydrophobic barrier to drop advancement. The surfactant molecule, with its hydrophile bound to the substrate, may pin the drop at the contact line joining the leading edge of the drop and pre-existing water film. The kinetics of desorption of the surfactant hydrophile from the substrate may govern the spreading rate. Surfactant aggregates may adsorb on hydrophilic substrates intact as there is no driving force to adsorb the hydrophobes on these surfaces. Consequently, aggregate disintegration may be slower than on hydrophobic substrates. (b) On surfaces of intermediate surface energy a pre-existing water layer necessary for Marangoni flow is still likely, but the tendency for the hydrophobe of the surfactant to adsorb to the substrate will increase. This can instigate aggregate disintegration, resulting in the efficient delivery of surfactant to the air-water interface when this occurs in the vicinity of the leading edge of the advancing drop. This is illustrated here for a flat layered microstructure unraveling at the leading edge, although the specific microstructure of the aggregates responsible for enhanced spreading have not been identified. Direct surfactant adsorption on the substrate in the region just beyond the contact line between the advancing drop and pre-existing water layer, depicted here by the arrow, will also reduce the concentration of surfactant at the opposing air-water interface and augment the surface tension gradient between these regions. The difference in thickness of the pre-existing water layer in (a) and (b) is only for clarity. (c) On a highly hydrophobic substrate a pre-existing water layer is considerably less likely, prohibiting the creation of the surface tension gradient necessary for Marangonic flow. Very hydrophobic surfaces do not favor formation of a continuous water film, which prevents the creation of the surface tension gradient necessary for Marangoni flow and accounts for the negligible spreading on these surfaces. Spreading on these surfaces also is less thermodynamically favorable owing to a less positive spreading coefficient.

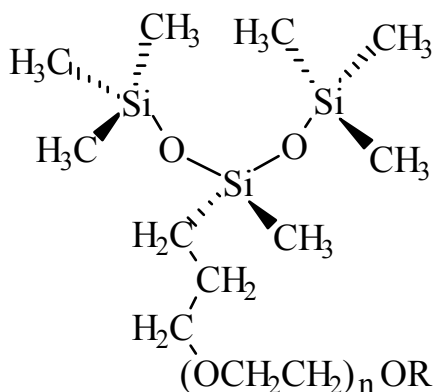
### Publications

- Determination of Wetting Velocities of Surfactant Superspreaders with the Quartz Crystal Microbalance, Z. Lin, R. M. Hill, H. T. Davis, and M. D. Ward, *Langmuir*, **1994**, *10*, 4060.
- Improved Accuracy in Dynamic Quartz Crystal Microbalance Measurements of • Surfactant Enhanced Spreading, Zuxuan Lin, T. Stoebe, Randal M. Hill, H. Ted Davis, and Michael D. Ward, *Langmuir*, **1996**, *12*, 345.

The radial sensitivity of the quartz crystal microbalance (QCM), comprising an AT-cut quartz crystal coated with gold electrodes, was exploited for the measurement of wetting rates of

aqueous dispersions of a trisiloxane surfactant exhibiting "superspreading" behavior on different surfaces. The rate at which a droplet advances across the QCM surface was measured directly from the frequency transient accompanying radial spreading of the drop from the center of the quartz crystal to the periphery. This method provides for convenient measurement of spreading rates under a variety of conditions, allowing systematic investigations of the wetting behavior dependence on surfactant concentration, substrate surface energy, and humidity. The substrate surface energy can be adjusted readily by the preparation, on the gold electrodes of the QCM, of self-assembled single component or mixed organosulfur monolayers with judiciously chosen chemical functionalities at the termini of the alkyl chains. The surfactant concentration at which the maximal spreading velocity occurred was independent of substrate surface energy, indicating that the spreading rate was dependent upon the microstructure of the surfactant dispersion rather than the energetics of the solution/substrate interface. These studies also revealed a surprising dependence of the wetting velocity on surface energy in which the velocities were greatest on surfaces of moderate hydrophobicity. Previous work indicated that superspreading required a humid environment, suggesting that a thin film of water on the hydrophobic surface was required. The studies described here revealed significant water condensation on rough hydrophobic QCM surfaces compared to smooth hydrophobic surfaces, which is attributable to capillary condensation on the rough surfaces. Consequently, superspreading was observed on rough surfaces of high hydrophobicity, but is negligible on smooth ones. The resolution of the preexisting water film issue, and the heretofore undiscovered influence of surface energy on superspreading, demonstrated the utility of the QCM for measurements of dynamic wetting behavior.

These studies were followed by an improvement in the methodology which provided for more accurate spreading rates. The modification involved larger QCM electrodes, which increased the area over which the spreading event was measured compared to previously used smaller electrodes, and a frequency counter capable of more rapid data acquisition. The larger electrodes permitted spreading to be measured for longer times over a larger area relative to the initial drop size, while faster data acquisition provided more data immediately following introduction of the droplet to the QCM surface. This obviated overweighting of data acquired in the later stages of spreading when the aqueous film approached the electrode edges and advanced along the electrode tabs. These wetting rates were corroborated by real-time video microscopy of the wetting processes on identical surfaces. Comparison of the wetting rates on gold electrodes modified with various organosulfur monolayers revealed that the dependence of rates on surface energy is identical for the different electrode sizes, the rates being systematically larger for the larger electrodes.



## M(D'E<sub>n</sub>OH)M

- Surfactant Enhanced Spreading, T. Stoebe, Zuxuan Lin, Randal M. Hill, H. Ted Davis, and Michael D. Ward, *Langmuir*, **1996**, *12*, 337.

The spreading of aqueous mixtures of a number of surfactants, including “superspreading” trisiloxane surfactants, has been investigated as a function of surfactant concentration, substrate surface energy, temperature, humidity, and substrate roughness. The substrate surface energy, characterized in terms of the contact angle of water, was controlled by the deposition of mixed organosulfur monolayer with different terminal chemical functionalities. The data demonstrates a strong spreading rate dependence on both surfactant concentration and surface energy. Furthermore, they indicated that nonturbid trisiloxane surfactant solution, which were previously believed not to promote rapid spreading, display superspreading characteristics, albeit on substrates which were less hydrophobic than those initially investigated. Moreover, both turbid dispersions and nonturbid solution of nonionic surfactants lacking trisiloxane groups have also been found to promote greatly enhanced spreading on less hydrophobic surfaces. Cationic and anionic surfactants were not observed to exhibit enhanced spreading characteristics. These results indicate that surfactant enhanced spreading, denoted earlier as “superspreading,” is not limited to turbid aqueous dispersions of trisiloxane surfactants, and this phenomenon may be more general and occur in a much more diverse class of compounds than previously thought.

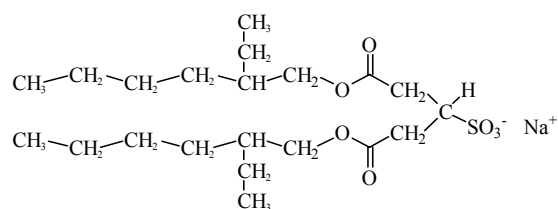
- Enhanced Spreading of Aqueous Ethoxylated Alcohol Surfactant Systems on Solid Substrates, T. Stoebe, Zuxuan Lin, Randal M. Hill, Michael D. Ward, and H. Ted Davis, *Langmuir* **1997**, *13*, 7270.

The spreading behavior of aqueous solutions containing the ethoxylated alcohol surfactants  $\text{CH}_2(\text{CH}_2)_9(\text{OCH}_2\text{CH}_2)_3\text{OH}$  and  $\text{CH}_3(\text{CH}_2)_{11}(\text{OCH}_2)_n\text{-OH}$  ( $n=3-6$ ) on solid substrates has been investigated at different surfactant concentrations and substrate surface energies. The trends in the dynamic spreading behavior differ from those expected based on the thermodynamic spreading coefficients calculated from static surface tensions. The data demonstrate that the spreading rates do not depend upon any identifiable aqueous phase surfactant microstructure. However, the spreading rate dependence upon the length of the hydrophilic poly(oxyethylene) chain suggests an interplay between surfactant adsorption on the substrate surface and the aggregation of this surfactant. The results suggest that the onset of turbidity, and an optimal surfactant hydrophilic/hydrophobic balance, are important for achieving high spreading rates.

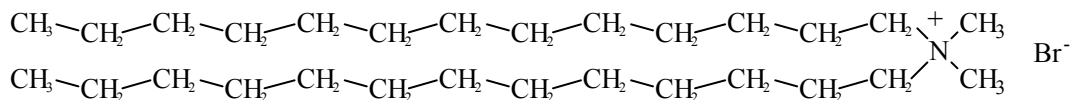
- Surfactant Enhanced Spreading of Aqueous Media Containing Ionic Surfactants, T. Stoebe, Randal M. Hill, Michael D. Ward, and H. Ted Davis, *Langmuir*, **1997**, *13*, 7276.

The spreading behavior of ionic surfactant aqueous systems on organosulfur monolayers with differing compositions and surface energies has been investigated. Aqueous solutions of the anionic surfactant sodium bis(2-ethylhexyl) sulfosuccinate (AOT) and the cationic surfactant

didodecyldimethyl ammonium bromide (DDAB) exhibit spreading characteristics that were previously thought to be reserved to non-ionic surfactant aqueous systems. These characteristics include rapid spreading over moderately hydrophobic substrates that are not wetted in the absence of surfactant, a maximum in spreading rate at intermediate substrate surface energies, and a maximum in spreading rate with respect to surfactant concentration (well above the respective critical micelle concentrations). Addition of coordinating alkali metal salts increased the spreading rates of AOT/H<sub>2</sub>O mixtures but reduced the spreading rates of the DDAB/H<sub>2</sub>O mixtures. Addition of non-coordinating salts did not significantly increase spreading rates of AOT/H<sub>2</sub>O mixtures but still resulted in reduced spreading rates of the DDAB/H<sub>2</sub>O mixtures. These results illustrate the complexity of the surfactant enhanced spreading process and support an important role for surfactant adsorption near the leading edge of the solid-liquid interface.



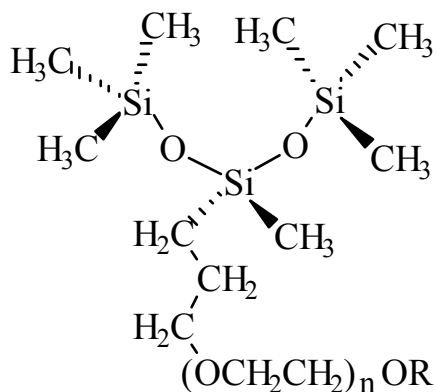
AOT



DDAB

- Superspreading of Aqueous Films Containing Trisiloxane Surfactant on Mineral Oil, T. Stoebe, Zuxuan Lin, Randal M. Hill, Michael D. Ward and H. Ted Davis, *Langmuir* **1997**, 13, 7282.

The spreading of water droplets, containing various surfactants, on liquid mineral oil surfaces has been investigated. Only "superspreading" trisiloxane surfactants were observed to promote rapid spreading on mineral oil, and the spreading characteristics of these systems differ substantially from those observed on solid substrates of comparable hydrophobicity. These differences include significantly faster spreading rates and monotonically increasing spreading rates with increasing surfactant concentration. Superspreading is attributed to Marangoni flow along the mineral oil-water interface. The extremely fast spreading on the mineral oil surface, as compared to hydrophobic solid surfaces, is attributed to the absence of the no-slip condition at the mineral oil-water interface. Real-time videomicroscopy of the spreading of aqueous droplets containing the trisiloxane surfactant M(D'E<sub>4</sub>OH)M revealed stepwise motion of the leading edges of the aqueous drop driven by disintegration of large surfactant aggregates at the mineral oil-water interface. This observation suggests that disintegrating aggregates instantaneously deliver large amounts of surfactant to the mineral oil-water interface, creating large surface tension gradients that are required for Marangoni flow. These results imply an important role of aggregate disintegration during the spreading of surfactant dispersions on hydrophobic solid substrates.



M(D'E<sub>n</sub>OH)M

- Surfactant Enhanced Spreading, T. Stoebe, Randal M. Hill, Michael D. Ward, L. E. Scriven and H. Ted Davis, "Silicone Surfactants," *Surfactant Science Series*, in press.

Recent studies of the wetting and spreading behavior of aqueous surfactant solutions and dispersions on solid substrates are reviewed. A diverse variety of non-ionic and a limited number of ionic surfactants enhance the spreading of aqueous films over relatively hydrophobic surfaces. The spreading rates depend strongly on surfactant concentration, substrate surface energy, roughness, and, in some cases, relative humidity. The data suggest that surface tension gradients (Maragoni flow) and surfactant adsorption on the substrate surface conspire to enhance the spreading of aqueous solutions. The generality demonstrated by the variety of surfactants exhibiting this behavior provides insight into the spreading mechanism and portends significant advances in surfactant formulations for coatings, cosmetics and agricultural adjuvants.